2007

RKEM implementation for strain gradient theory in multiple dimensions

Abhishek Kumar
University of South Florida

RKEM Implementation for Strain Gradient Theory in Multiple Dimensions

by

Abhishek Kumar

A thesis submitted in partial fulfillment
of the requirements for the degree of
Master of Science in Engineering
Department of Civil and Environmental Engineering
College of Engineering
University of South Florida

Major Professor: Daniel Simkins,Ph.D.
Andres Tejada Martinez, Ph.D.
Muhammad Mustafizur Rahman, Ph.D.

Date of Approval:
July 11, 2007

Keywords: couple stress, bimaterial, higher order diffrential equation, messless, isogeometric

Dedication

This work is dedicated to my mother Late Usha Sharma, whose presence i always felt in whatever i did

Acknowledgments

I would like to thank Prof. Simkins for giving me an opportunity to work under his guidance. Prof. Simkins has played a very important role in helping me with my thesis work, without his time endless encouragement and patience this work would not have been possible. I thank Prof. Tezada and Prof Rahman for time they took to review this thesis and there valuable suggestion to improve it. I am indebted to the support and encouragement I have got from my family, friends and colleagues.

Table of Contents

List of Figures

RKEM Implementation for Strain Gradient Theory in Multiple Dimensions

Abhishek Kumar

ABSTRACT

The Reproducing Kernel Element Method (RKEM) implementation of the Fleck-Hutchinson phenomenological strain gradient theory in 1D, and higher dimension is implemented in this research. Fleck-Hutchinson theory fits within the framework of Touplin-Mindlin theories and deals with first order strain gradients and associated work conjugate higher-order stress. Theories at the intrinsic or material length scales find applications in size dependent phenomena. In elasticity, length scale enters the constitutive equation through the elastic strain energy function which depends on both strain as well as the gradient of rotation and stress. The displacement formulation of the Touplin Mindlin theory involves diffrential equations of the fourth order, In conventional FEM C^1 elements are required to solve such equations. C^1 elements are cumbersome in 2D and unknown in 3D. The high computational cost and large number of degrees of freedom soon place such formulation beyond the realm of practicality.

Recently, some mixed and hybrid formulations have been developed which require only C^0 continuity but none of these elements solve complicated geometry problems in 2D and there is no problem yet solved in 3D. The large number of degrees of freedom is still inevitable for these formulations. As has been demonstrated earlier RKEM has the potential to solve higher-order problems, the degree of freedom consist of nodal displacement and their derivatives. This method has the promise to solve important problems formulated with higher order derivatives, such as The strain gradient theory.

Chapter 1

Introduction

Classical (local) continuum constitutive models possess no material/intrinsic length scale. The typical dimensions of length that appear in the corresponding boundary value problems are associated with the overall geometry of the domain under consideration. In spite of the fact that classical theories are quite sufficient for most applications, there is ample experimental evidence which indicates that, in certain applications, there is significant dependence on additional length/size parameters. Some of these instances, as selected from the literature, include the dependence of the initial flow stress upon particle size, the dependence of hardness on size of the indenter, the effect of wire thickness on torsional response, the development and evolution of damage in concrete, etc. All these investigations highlight the inadequacy of local continuum models in explaining the observed phenomena, thereby motivating the need to introduce non-local continuum models that have length scales present in them. An extensive summary of this experimental evidence is given in a recent review article by Fleck and Hutchinson [9]. In "gradient-type" plasticity theories, length scale is introduced through the coefficient of spatial gradients of one or more internal variables. In elasticity, length scale enters the constitutive equation through the elastic strain energy function, which in this case depends not only on the strain tensor but also on gradients of the rotation and strain tensor.

Conventional continuum mechanics theories assume that stress at a material point is a function of 'state' variables, such as stress at the same point. This local assumption has long been proved to be adequate when the wavelength of the deformation field is much larger than the micro-structural length scale of the material. However when the two length scales are comparable, the assumption is questionable as the material behavior at a point is influenced by deformation of neighboring points. Starting from the pioneering Cosserat couple stress theory [3], various non-local or strain gradient continuum theories have been proposed. In the full Cosserat theory [3], an independent rotation quantity θ is defined in addition to the material displacement $\mathbf{u}$; couple stresses (bending moment per unit area) are introduced as the work conjugate to the micro-curvature (that is, the spatial gradient of θ). Later, Toupin [29] and Mindlin [22] proposed a more general theory which includes not only micro-curvature, but also gradients of normal strain. Both the Cosserat and Toupin-Mindlin theories were developed for linear elastic materials. Afterwards, non-local theories for plastic materials

was developed by, among others, Aifantis [7] and Fleck and Hutchinson [8, 9]. Fleck-Hutchinson strain gradient plasticity theories fall within the Touplin -Mindlin framework. Interest in non-local continuum plasticity theories have been rising recently due to an increasing number of observed size effects in plasticity phenomena. Variants of this strain gradient plasticity theory have also appeared [11, 14, 31]. These theories have been widely applied to studying length scale-dependent deformation phenomena in metals. Polar and higher-order continuum theories have been applied to layered materials, composites and granular media, in addition to polycrystalline metals.

The solution of the initial and boundary value problems posed in terms of the higher-order theories is not straight forward: the governing differential equation and boundary conditions are complicated [29] and analytical solutions are restricted to the simplest cases. Computational difficulties also arise. While boundary conditions are easier to treat in the variational setting, requirements of regularity dictates that the displacement must be a C^1 function over the domain. The degrees of freedom include nodal displacement and displacement gradients. The situation is partially analogous to classical Bernoulli-Euler beam and Poisson-Kirchhoff plate theories in one and two spatial dimension respectively.

A finite element formulation incorporating C^1 displacement fields are therefore a natural first choice for strain gradient theories. For example, the use of Specht's triangular element [27] for the special case of couple stress theory was examined [32]. The element contains displacement derivatives as extra nodal degrees of freedom and C^1 continuity is satisfied only in a weak averaged sense along each side of the element; therefore the element is not a strict C^1 element. Furthermore, the element fails to deliver an accurate pressure distribution for an incompressible, non linear solid. There is a rectangular C^1 element [23], but its shape and number of degrees of freedom are strong limitation for its implementation in two and higher dimensional problems. As is easily appreciated, the computational cost is high; the large number of degrees of freedom soon place such formulation beyond realm of practicality.

The lack of robust C^1-continuous elements then motivated the development of various C^0-continuous elements for couple stress theory in recent decades([32], [15], [30] [6] [33], [21] [18] etc). Finite element formulations for the Fleck-Hutch strain gradient plasticity theory have been developed with plate elements as a basis, but were generally found to perform poorly [32]. Mixed and hybrid formulations have also been developed in the same work and elsewhere the work of [30] introduced some C^0 element types, where nodal degrees of freedom include nodal displacement and corresponding gradients, and the kinematic constraint between displacement and displacement gradient are enforced via the Lagrange multiplier method. Their lowest order triangular element requires 28 unknowns per element, and their lowest order quadrilateral ele-

ment 38 unknowns; Amanatidou and Aravas [6] proposed mixed C^0 -continuity finite element formulations, where every element includes around 70 nodal degrees of freedom in 2-D problems. G.Engel et. al. [21] tries to solve the same problem using a continuous/discontinuous finite element approximation. In this work they have presented rate of convergence and error estimates derived for energy and L^2 norms. But this has been limited to 1D problems and to the best of the author's knowledge there is no extension of this formulation to two and higher dimension. From this information it is evident that currently no finite element method nor extensions of finite element methods is available for strain gradient theory formulation in higher dimensions.

During the last two decades, the technique of meshless interpolation of trial and test functions has been attracting great attention. Meshfree methods such as the hp-cloud method [2], the method of finite spheres [4], the particle partition of unity method [13], reproducing kernel particle methods [**?**] , the element free Galerkin method [28], the finite point method [5], the diffuse element method [1], the modified local Petrov-Galerkin method [26], smooth particle hydrodynamics [20], among others, offer an attractive alternative for solution of many classes of problem that are difficult or even not feasible to solve using the finite elements because these methods posess intrinsic non-local properties. Unlike a typical finite element method, the nonlocal properties of meshfree approximations confer an arbitrary degree of smoothness on solutions and have been applied to various problems.

The Reproducing Kernel Element Method(RKEM) first presented by Liu et al.is the first globally compatible, minimal degree of freedom, arbitrary degree of continuity basis function on a given mesh. The salient feature of RKEM is the hybridization of finite element shape functions with the mesh free kernel function. Detailed formulation for RKEM is given in section 3. Use of RKEM to solve plate and shell structures problem which contain higher order differential derivative has been demonstrated . In this work, the detail review of strain gradient theory is given in chapter 2. The application of RKEM to strain gradient theory is discussed in detail in chapter 3 and 4. To study the accuracy of the present method, convergence test are carried out and several problems in one and two dimensions are analyzed in chapter 5 and 6. From these tests, the RKEM method is found to give quite accurate results. The remarkable accuracy in these numerical simulations show promising characteristics for solving general problems for materials whose constitutive law involve strain-gradients.

Chapter 2

Review of Linear Elastic Strain Gradient Theory

Touplin [29] and Mindlin [22] developed a theory of linear elasticity whereby the strain energy density per unit volume($\mathbf{w}$) depends upon both the strain $\epsilon_{ij} \equiv (u_{i,j} + u_{j,i})/2$ and strain gradient $\eta_{ijk} \equiv u_{k,ij}$. Here $\mathbf{u}$ is the displacement field and comma represents partial differentiation with respect to a Cartesian co-ordinate. In addition to the Cauchy stress σ_{ij} , this theory also takes into account higher order stress τ_{ijk} which is work conjugate to η_{ijk}.

Due to the symmetric property of strain tensor $\epsilon_{ij} = \epsilon_{ji}$.

The strain energy function $\mathbf{w}$ is assumed to be a convex function, with respect to its argument(ϵ, η) for each point x of a solid of volume V. The total energy W stored in the solid is determined by the displacement field $\mathbf{u}$(x) within V

$$W(u) \equiv \int_V w(\epsilon(u), \eta(u); x)\, dx \tag{1}$$

with ϵ , η being derived from $\mathbf{u}$, as discussed above.

The energy variation of the solid due to an arbitrary variation of the displacement $\mathbf{u}$ is :

$$\delta W = \int_V (\sigma_{ij}\delta\epsilon_{ij} + \tau_{ijk}\delta\eta_{ijk})\, dx. \tag{2}$$

Mindlin [22] showed that for a general isotropic linear hyper-elastic material the solid strain energy per unit volume($\mathbf{w}$) can be expressed as

$$w = \frac{1}{2}\lambda\epsilon_{ii}\epsilon_{jj} + \nu\epsilon_{ii}\epsilon_{jj} + a_1\eta_{ijj}\eta_{ikk} + a_2\eta_{iik}\eta_{kjj} + a_3\eta_{iik}\eta_{jjk} + a_4\eta_{ijk}\eta_{ijk} + a_5\eta_{ijk}\eta_{jki} \tag{3}$$

in terms of the invariants of the second-order strain tensor and the third-order strain gradient tensor. Here λ and ν are the standard Lame constants and the five a_n are additional constants of dimensions of stress times length squared.

From the constitutive law the stress σ_{ij} and the higher order stress η_{ijk} for an elastic solid is derived as :

$$\sigma_{ij} = \frac{\partial w}{\partial \epsilon_{ij}}$$

and

$$\tau_{ijk} = \frac{\partial w}{\partial \eta_{ijk}}$$

For Linear Elasticity σ_{ij} and η_{ijk} can be written as

$$\sigma_{ij} = \frac{\partial w}{\partial \epsilon_{ij}} = 2\nu\epsilon_{ij} + \lambda\epsilon_{kk}\delta_{ij} \tag{4}$$

$$\eta_{ijk} = \frac{\partial w}{\partial \eta_{ij}} = a_1(\eta_{ipp}\delta_{jk} + \eta_{jpp}\delta_{ik} + a_2(\eta_{kpp}\delta_{ij} + \frac{1}{2}\eta_{ppi}\delta_{jk} + \frac{1}{2}\eta_{ppj}\delta_{ik} + a_3(2\eta_{ppk}\delta_{ij}) + a_4(2\eta_{ijk}) + a_5(\eta_{jki} + \eta_{ikj}) \tag{5}$$

The principal of virtual work can be expressed as [9]

$$\int_V [\sigma_{ij}\delta\epsilon_{ij} + \tau_{ijk}\delta\eta_{ijk}]dV = \int_v [b_k\delta u_k]dV + \int_s [f_k\delta u_k + r_k D\delta u_k]dS \tag{6}$$

for an arbitrary displacement increment δu. Here b_k is the body force per unit volume of the body V while f_k and r_k are the traction and double stress traction per unit area of the surface S, respectively. They are in conjunction with the Cauchy stress σ_{ij} and higher order stress τ_{ijk} according to

$$b_k + (\sigma_{ik} - \tau_{jik,j})_{,i} = 0 \tag{7}$$

$$f_k = n_i(\sigma_{ik} - \tau_{jik,i}) + \eta_i\eta_j\tau_{ijk}(D_p\eta_p) - D_j(\eta_i\tau_{ijk}) \tag{8}$$

and

$$r_k = \eta_i\eta_j\tau_{ijk} \tag{9}$$

In the above equation $D_j(\cdot) = (\delta_{jk} - \eta_j\eta_k)\frac{\partial(\cdot)}{\partial x_k}$ is a surface gradient operator and $D(\cdot) = \eta_k\frac{\partial(\cdot)}{\partial x_k}$ is surface normal-gradient operator. n_i is the ith componenent of the unit surface normal operator. The strain gradient theory dictates that, in order to have a unique solution, six boundary conditions must be independently

prescribed at any point on the surface of the body , i.e. f_k or u_k, and r_k or $\mathrm{D}u_k$. The extra boundary conditions on r_k or $\mathrm{D}u_k$ are characteristic of the strain gradient theory and, as can be seen later in one particular example, they imply strain continuity across the interface between two dissimilar materials.

Chapter 3

Review of RKEM

A new class of method, the Reproducing Kernel Element Method(RKEM) [17] , [16] [19], [24] has been recently developed. This method takes salient features from the FEM and meshfree methods. The essence of RKEM is to extend the notion of the FEM element shape functions to the entire domain and use a meshfree kernel to combine them in such a way as to ensure global compatibility, partition of unity and global reproducing properties.

3.1 Concept of RKEM

The RKEM method is illustrated briefly in this section.

As the name implies, RKEM is an element based method not like meshless methods. An element is a subset of the domain of the problem. The solution is represented as a linear combination of shape or basis functions on the domain. The shape functions are associated with nodal degrees of freedom (DOF) at each node, which are related to the primary unknowns and its various derivatives. For each DOF associated global partition polynomials are constructed. Unlike the construction of high order finite element shape functions, the RKEM shape function does not need any extra degrees of freedom either on the side of the element or in the interior. The requirement on the number of degrees of freedom is absolutely minimum.

The RKEM is developed to achieve these following objectives:

1. No numerically induced discontinuity between elements. Inter-element boundary continuities limit the smoothness of FEM shape function. For example, to solve a fourth order differential equation, one needs C^1 elements in a standard conforming method. In practice it is very difficult to get continuity between two such element in two or higher dimensional domains. RKEM is developed to overcome this difficulty.

2. No special treatment required for enforcing essential boundary conditions. For most meshfree methods, the treatment of Dirichlet boundary conditions is problematic due to loss of the Kronecker delta

property of meshfree shape functions. The treatment of Dirichlet boundary conditions in RKEM is straightforward.

3. High order smooth interpolation in arbitrary domains of multiple dimensions.

RKEM shape functions are formed by combining global partition polynomials and the meshfree reproducing kernel functions. Global partition polynomials (gpp) for RKEM have the same properties as those of FEM, but they are defined globally. Detailed formulation of gpp's are given in the next section in this chapter. It should be noted that the gpp's are always constructed to be Hermite polynomials. Kernel functions are used to truncate the gpp's outside a compact support such that the reproducing conditions are satisfied. The term reproducing condition refers to ability of shape function to reproduce a constant, as part of the requirements for convergence.

An RKEM interpolation field is defined as:

$$If(\mathbf{x}) = \sum_{e=1}^{N_{elem}} \left[\int_{\Omega_e} K_\rho(\mathbf{x}-\mathbf{y}:\mathbf{x})\mathbf{dy} \left(\sum_{\mathbf{i=1}}^{\mathbf{nnodes}} \psi_{\mathbf{e,i}}(\mathbf{x})\mathbf{f}(\mathbf{x_{e,i}}) \right) \right] \tag{10}$$

where f($\mathbf{x}$) is the interpolated function; K_ρ is the meshfree kernel function; N_{elem} is the number of elements in the domain; nnodes is the number of nodes for a particular element, e.g. nnodes =3 for a triangular element; Ω_e is element domain, $\psi_{e,i}(\mathbf{x})$ are the global partition polynomials; and I is the interpolation operator.

After nodal integration Eq. 10 can be written as

$$I^h f(\mathbf{x}) = \underset{e\in\bigwedge_E}{\mathbf{A}} \left[\left(\sum_{j=1}^{nnodes} K_\rho(\mathbf{x}-\mathbf{x}_{e,j}:\mathbf{x})\Delta V_{e,j} \right) \left(\sum_{i=1}^{nnodes} \psi_{e,i}(\mathbf{x}) f(\mathbf{x}_{e,i}) \right) \right] \tag{11}$$

where $\Delta V_{e,j}$ is the nodal integration weight, the Lobatto quadrature rule [12] [16] is used to assign this weight. The symbol $\underset{e\in\bigwedge_E}{\mathbf{A}}$ is the assembly operator and denotes the summation over the set of elements, ($\bigwedge_E$ of the mesh.

The reproducing kernel function is a function with compact support and is chosen to have the form

$$K_\rho = \frac{1}{\rho_{e,j}^d} w\left(\frac{\mathbf{x}-\mathbf{x_{e,j}}}{\rho_{e,j}} \right) b(\mathbf{x}) \tag{12}$$

where ρ is the support radius, d is the spatial dimension, $\mathbf{x}$ is the point at which the kernel is evaluatedd, w is a compactly-supported smooth window function, and the factor $b(\mathbf{x})$ is used for normalization. A smooth

window function $C^n(\Omega)$ is chosen to serve as the core of the kernel. In the present work, w in one dimension is taken to be a cubic spline, which gives C^2 continuity.

If $f(\mathbf{x})$ = 1 in Eq. 11 then we have

$$1 = \underset{e\in\bigwedge_E}{\mathbf{A}} \left[\left(\sum_{j=1}^{nnodes} \frac{1}{\rho_{e,j}^d} w\left(\frac{\mathbf{x}-\mathbf{x}_{e,j}}{\rho_{e,j}}\right) b(\mathbf{x}) \boldsymbol{\Delta}\mathbf{V}_{\mathbf{e,j}} \right) \left(\sum_{i=1}^{nnodes} \psi_{e,i}(\mathbf{x}) \right) \right] \tag{13}$$

Since the global partition polynomials for a single element are a partitions of unity Ω_e , i.e:

$$\left(\sum_{i=1}^{nnodes} \psi_{e,i}(\mathbf{x}) \right) = 1$$

we have

$$\underset{e\in\bigwedge_E}{\mathbf{A}} \left\{ \left(\sum_{j=1}^{nnodes} \frac{1}{\rho_{e,j}^d} w\left(\frac{\mathbf{x}}{-}\mathbf{x}_{e,j}\rho_{e,j}\right) b(\mathbf{x}) \Delta V_{e,j} \right) \right\} = 1 \quad \forall \mathbf{x} \in \Omega$$

The expression for the normalizer b($\mathbf{x}$) can be written using above equation as :

$$b(\mathbf{x}) := \left\{ \underset{e\in\bigwedge_E}{\mathbf{A}} \left[\left(\sum_{j=1}^{nnodes} \frac{1}{\rho_{e,j}^d} w\left(\frac{\mathbf{x}-\mathbf{x}_{e,j}}{\rho_{e,j}}\right) \Delta V_{e,j} \right) \right] \right\}^{-1} \tag{14}$$

Using the connectivity relation, the shape function ($\Psi_I(\mathbf{x})$) for RKEM at node I can be written as

$$\Psi_I(\mathbf{x}) = \sum_{k=1}^{l} \left(\sum_{j\in\bigwedge_{e_k}} \frac{1}{\rho_{e,j}^d} w\left(\frac{\mathbf{x}-\mathbf{x}_{e,j}}{\rho_{e,j}}\right) \Delta V_{e,j} \right) b(\mathbf{x}) \psi_{e_k,i_k}(\mathbf{x}) \tag{15}$$

and the reproducing kernel element interpolation in term of RKEM shape function can be written as

$$I^h f(\mathbf{x}) = \sum_{I=1}^{N_{nodes}} \Psi_I(\mathbf{x}) f_I \tag{16}$$

where N_{nodes} is total number of nodes for domain.

The RKEM shape functions are Generalized Hermite Functions, these are a set of functions, not necessarily polynomials which satisfies the interpolation condition

$$P^k(\xi_i) = y_i, \quad k = 0, 1, \cdots, n_i - 1, \quad 1 = 0, 1, \cdots, m \tag{17}$$

where P is polynomial and y_i is value of polynomial at ξ_i, i.e. Hermite interpolation interpolates not only the primary variable, but also the first n_i - 1 derivatives.

We will denote the RKEM domain by Ω throughout this thesis.

3.2 Global Partition Polynomial

The construction of global partition polynomials for RKEM is similar to that of FEM, except that it is defined globally instead of locally in FEM. The systematic procedure to construct the global partition polynomial is given in [25]. In this section the global partition polynomial for the element used in this work, the so called L4P3I1 and T9P2I1 will be discussed. The nomenclature L4P3I1 stands for Linear element which has 4 degrees of freedom, globally reproduces 3rd order Polynomials and Interpolates 1st order derivatives and T9P2I1 stands for Triangular element which has 9 degrees of freedom, globally reproduces 2nd order Polynomials and Interpolates 1st order derivatives.

3.2.1 The L4P3I1 Element

For one dimensional elements, the global partition polynomials are particularly easy. Depending on the order of interpolation, one uses the appropriate Hermite interpolant. The L4P3I1 element is constructed using the first order Hermite polynomials.

First order Hermite polynomials on an interval of length Δx_e with $\xi \in$ [0,1] are:

$$H_1^0(\xi) = 1 - 3\xi^2 + 2\xi^3 \tag{18}$$

$$H_2^0(\xi) = 3\xi^2 - 2\xi^3) \tag{19}$$

$$H_1^1(\xi) = \Delta x_e(\xi - 2\xi^2 + \xi^3) \tag{20}$$

$$H_2^1(\xi) = \Delta x_e(\xi^3 - \xi^2) \tag{21}$$

$$\tag{22}$$

The global partition polynomials for this element are the same as the standard FEM beam element shape functions. The shape function Ψ^{00} and Ψ^{10} for this element is shown in Fig. **??** and Fig. **??**

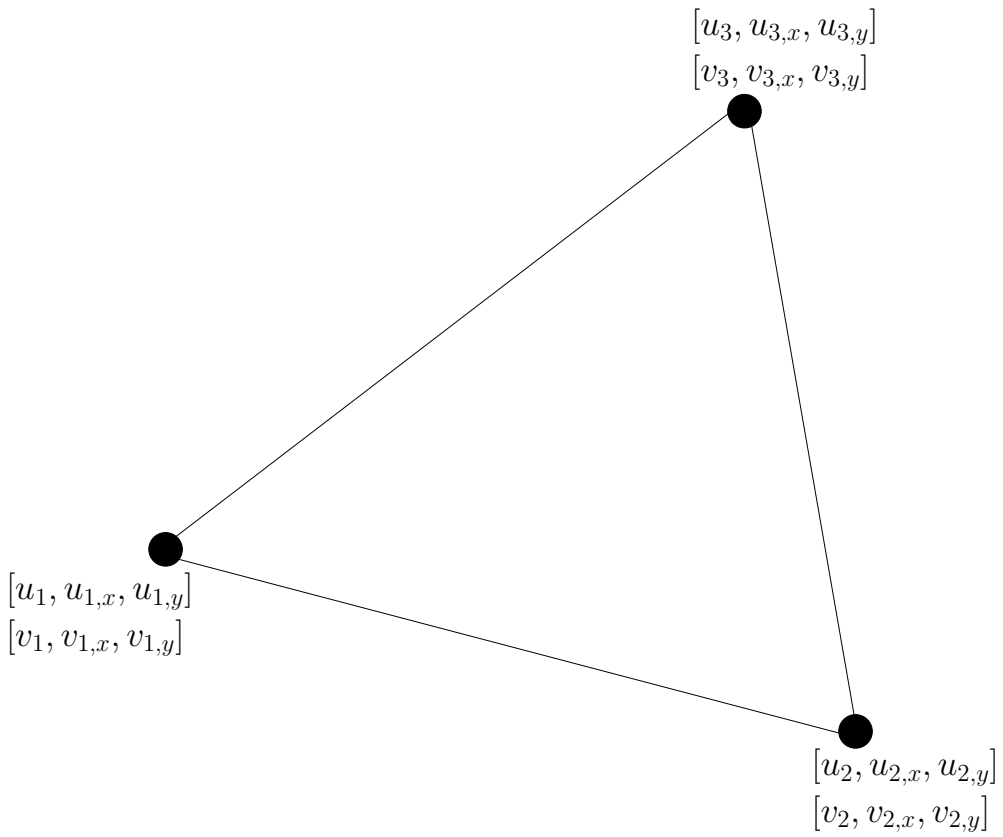

Figure 1. The T9P2I1 element with variable associated at each nodes

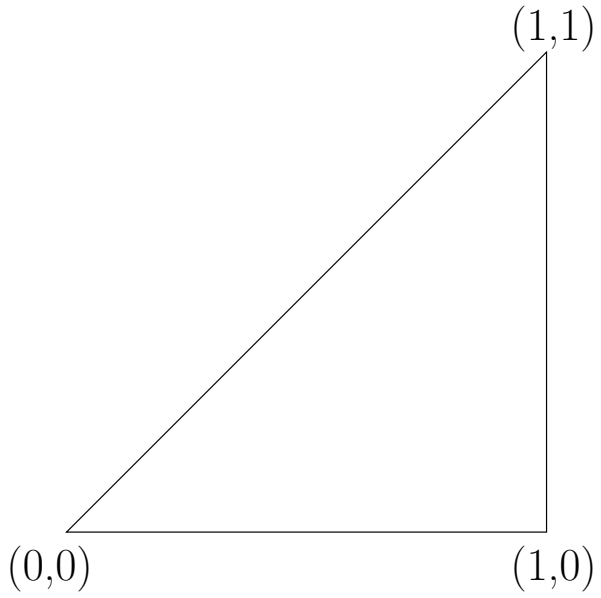

Figure 2. The parent triangle for T9P2I1 element

3.2.2 The T9P2I1 Element

The triangular element used in this work is the T9P2I1. In Fig. 1 the solid circle in triangle represents the node, nodal degrees of freedom associated with each node is given at each vertex, u and v represent displacement in x and y direction respectively.

As mentioned previously in this section, the smoothness or continuity of the global RKEM shape function is determined by the continuity of the reproducing kernel, a third order spline is used as the window function for this element. Therefore, the element is a global C^2 compatible element. The element has 9 degrees of freedom, the global partition polynomials are constructed using the parametric approach. In the parametric approach the geometric(physical) triangle shown in Fig. 1 is mapped to a parent triangle shown in Fig. 2.

The reason for choosing this parent triangle is explained in [25].

The shape function for this parent triangle are:

$$N_1(s,t) = 1 - s \tag{23}$$

$$N_1(s,t) = s - t \tag{24}$$

$$N_1(s,t) = t \tag{25}$$

The global partition polynomials are derived by considering the following element interpolation field in a three node triangular parent element (e),

$$If = \sum_{i=1}^{3} \left(\psi_{e,i}^{(00)}(\mathbf{x}) f_{e,i} + \psi_{e,i}^{(10)}(\mathbf{x}) \left.\frac{\partial f}{\partial x}\right|_{e,i} + \psi_{e,i}^{(01)}(\mathbf{x}) \left.\frac{\partial f}{\partial y}\right|_{e,i} \right) = \mathbf{\Psi^T f} \tag{26}$$

where ψ is denoted as the local shape function array and vector f is nodal data array, i.e.

$$\psi^T := \left[\psi_{e,1}^{00} \quad , \psi_{e,1}^{10} \quad , \psi_{e,1}^{01} \quad , \psi_{e,2}^{00} \quad , \psi_{e,2}^{10} \quad , \psi_{e,2}^{01} \quad , \psi_{e,3}^{00} \quad , \psi_{e,3}^{10} \quad , \psi_{e,3}^{01} \right] \tag{27}$$

$$\mathbf{f}^T := \left[f_{e,1} \quad , f_{e,1_x} \quad , f_{e,1_y} \quad , f_{e,2} \quad , f_{e,2_x} \quad , f_{e,2_y} \quad , f_{e,3} \quad , f_{e,3_x} \quad , f_{e,3_y} \right] \tag{28}$$

Based on [25] the final result for the global partition polynomials for this parent element are:

$$\tilde{\psi}_1^{(00)} = 2s^3 - 3s^2 + 1 \tag{29}$$

$$\tilde{\psi}_1^{(10)} = s^3 - 2s^2 + s \tag{30}$$

$$\tilde{\psi}_1^{(01)} = \frac{1}{2}(st^2 + s^2t - t^2 - 3st) + t \tag{31}$$

$$\tilde{\psi}_2^{(00)} = 2t^3 - 2s^3 + 3s^2 - 3t^2 \tag{32}$$

$$\tilde{\psi}_2^{(10)} = \frac{1}{2}(t^2 - st^2 - s^2t + st) + s^3 - s^2 \tag{33}$$

$$\tilde{\psi}_2^{(01)} = t^3 - \frac{1}{2}(st^2 + s^2t + 3t^2 - 3st) \tag{34}$$

$$\tilde{\psi}_3^{(00)} = 3w^2 - 2w^3 \tag{35}$$

$$\tilde{\psi}_3^{(10)} = \frac{1}{2}(sw^2 + s^2w - w^2 - ws) \tag{36}$$

$$\tilde{\psi}_3^{(01)} = \frac{1}{2}(tw^2 + t^2w - w^2 - wt) \tag{37}$$

$$\tag{38}$$

The global RKEM interpolation field is constructed based on the Eq. 15. Quadratic Polynomials are reproduced using these shape functions. The shape and profile of the global RKEM shape function of this element is displayed in Fig. 3. It is important to note that each plot is scaled for visibility, thus relative magnitudes cannot be determined from the plots. The shape of the global interpolation function depends upon the mesh and node, whether it is a boundary node or it is in the interior of the domain. The shape functions plotted in Fig. 3 are computed for the middle node of the mesh shown in Fig. 9.

3.3 Salient Features of RKEM

The following are some salient features of RKEM which differentiates it from FEM and other meshless methods:

1. The shape functions are Generalized Hermite interpolants. As such, at each node the primary variable and various of its derivatives are interpolated. This property is useful in interpolating derivatives of primary variable, e.g. stresses in elasticity problems.

2. The shape functions possess the Higher-order Kronecker-δ property:

$$D^{\alpha}\Psi_I^{(\beta)}\Big|_{\mathbf{x}=\mathbf{x}_J} = \delta_{IJ}\delta_{\alpha\beta}, \quad \mathbf{x}_I,\, \mathbf{x}_J \in \bar{\Omega}, \;\; |\alpha|, |\beta| \leq m, \tag{39}$$

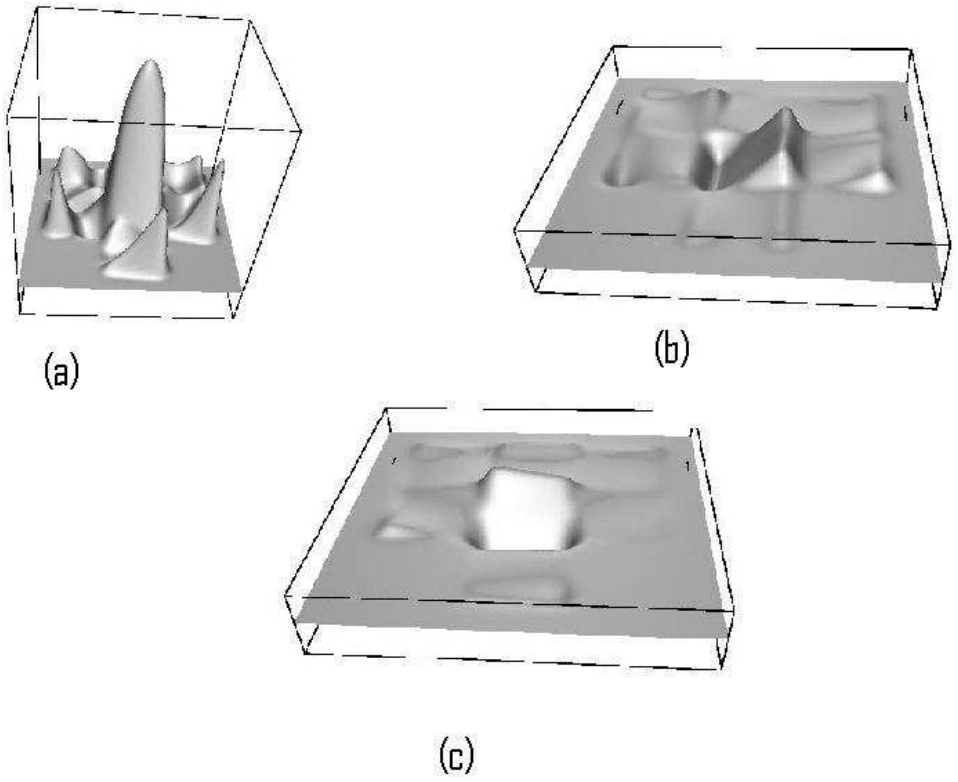

Figure 3. The global shape function of T9P2I1 element (a)$\Psi_1^{(00)}$, (b)$\psi_1^{(10)}$ (c)$\psi_1^{(01)}$

Index β means which derivative of shape function, e.g. in one dimension Ψ^{00} corresponds to $\beta = 0$ and Ψ^{10} correspond to $\beta = 1$, α is an integer the maximum value of which depends on highest order to which RKEM shape function is differentiable. I and x_j are node and coordinates respectively at which RKEM shape function are evaluated.

This property is helpful for treatment of Dirichlet boundary conditions, the majority of meshless methods have difficulty in imposing these boundary conditions.

3. The shape functions form a Partition of Unity: $\sum_I \Psi_I^\alpha(x) = 1 \quad \forall x \in \Omega; \quad |\alpha| = 0$. This helps to ensure consistency for RKEM kernel function

4. The shape functions possess the global reproducing property:

$$\sum_I \left\{ \sum_\alpha \Psi_I^\alpha(\mathbf{x})(D^\alpha \mathbf{x}^\beta)|_{\mathbf{x}=\mathbf{x}_I} \right\} = \mathbf{x}^\beta, \ \ \forall \, \mathbf{x} \in \Omega \tag{40}$$

5. Each shape function has compact support with fixed size, regardless of reproducing order. The support size is dependent solely on the topology of the RKEM mesh.This property make the stiffness matrix sparse,lending to economic formation and solution.

6. Smoothness: Given a kernel function that is C^n continuous, the resulting RKEM shape functions are also C^n. This property is useful for smooth geometry representation in computational geometry. ([25]).

To guarantee the above properties, RKEM meshes must satisfy a *quasi-uniformity* condition as discussed in [16]. In simple terms, this condition places some restriction on the aspect ratio of individual elements and the gradation of element sizes within the mesh.

Chapter 4

Galerkin Formulation for Strain Gradient Problems

The plane stress/strain assumption is taken in 2D examples in this research. In general, the displacement field for two dimensional problems are

$$u_i = u_i(x_1, x_2) \qquad i = 1, 2 \qquad u_3 = 0$$

strain and strain gradients are

$$\epsilon_{ij} = \frac{1}{2}(u_{i,j} + u_{j,i}) \qquad i = 1, 2: \qquad j = 1, 2 \tag{41}$$

$$\eta_{ij\gamma} = u_{\gamma,ij} \qquad \gamma = 1, 2 \tag{42}$$

and the corresponding conventional and higher order stresses are

$$\sigma_{ij} = \frac{\partial w}{\partial \epsilon_{ij}} = 2\nu\epsilon_{ij} + \lambda\epsilon_{kk}\delta_{ij} \tag{43}$$

$$\begin{aligned} \eta_{ijk} = a1(\eta_{ipp}\delta_{jk} + \eta_{jpp}\delta_{ik} + a2(\eta_{kpp}\delta_{ij} + \frac{1}{2}\eta_{ppi}\delta_{jk} \\ + \frac{1}{2}\eta_{ppj}\delta_{ik} + a3(2\eta_{ppk}\delta_{ij}) + a4(2\eta_{ijk}) + a5(\eta_{jki} + \eta_{ikj}) \end{aligned} \tag{44}$$

The equilibrium equation for strain gradient theory is given by Eq. 7, and the corresponding weak form for the problem is

$$\int_V [\sigma_{ij}\delta\epsilon_{ij} + \tau_{ijk}\delta\eta_{ijk}]dV = \int_v [b_k\delta u_k]dV + \int_s [f_k\delta u_k + r_k D\delta u_k]dS \tag{45}$$

For convenience, we assume the body force and body double force to be zero, due to this assumption the weak form becomes

$$\int_V [\sigma_{ij}\delta\epsilon_{ij} + \tau_{ijk}\delta\eta_{ijk}]dV = \int_s [f_k\delta u_k]dS \tag{46}$$

The unknown variable u(displacement in x direction) can be written in terms of RKEM shape functions as :

$$u(x) = \sum_{I=1}^{N_{nodes}} \left(\Psi_I^{00} u^I + \Psi_I^{00} u^I + \Psi_I^{00} u^I \right) \tag{47}$$

It is convenient to recast this in matrix form as

$$u(x) = \mathbf{Nu}$$

where

$$\mathbf{N} = [N_1 \; N_{1,x} \; N_{1,y} \; N_2 \; N_{2,x} \; N_{2,y} \; \cdots N_{N_{nodes}} \; N_{N_{nodes},x} \; N_{N_{Nodes},y}]$$

and

$$\mathbf{u}^T = [u_1 \; u_{1,x} \; u_{1,y} \; u_2 \; u_{2,x} \; u_{2,y} \; \cdots u_{N_{nodes}} \; u_{N_{nodes},x} \; u_{N_{Nodes},y}]$$

Similarly $\delta u(x) = \delta u^T N^T$,

For two dimensional problems strain and strain-gradient can be written in vector form as

$$\epsilon = \begin{bmatrix} \epsilon_{xx} \\ \epsilon_{yy} \\ \epsilon_{xy} \end{bmatrix} = \begin{bmatrix} u_{,x} \\ v_{,y} \\ (v_{,x} + u_{,y}) \end{bmatrix} \tag{48}$$

$$\eta = \begin{bmatrix} \eta_{xxx} \\ \eta_{xyx} \\ \eta_{yyx} \\ \eta_{xxy} \\ \eta_{xyy} \end{bmatrix} = \begin{bmatrix} u_{,xx} \\ u_{,xy} \\ u_{yy} \\ v_{xx} \\ v_{xy} \\ v_{yy} \end{bmatrix} \tag{49}$$

where v is displacement in y direction.

For the T9P2I1 element, the strain-displacement matrix ($\mathbf{B_i}$) for node i is given as

$$\mathbf{B_i} = \begin{bmatrix} \psi_{i,x}^{00} & \psi_{i,x}^{10} & \psi_{i,x}^{01} & 0 & 0 & 0 \\ 0 & 0 & 0 & \psi_{i,y}^{00} & \psi_{i,y}^{10} & \psi_{i,y}^{01} \\ \psi_{i,y}^{00} & \psi_{i,y}^{10} & \psi_{i,y}^{01} & \psi_{i,x}^{00} & \psi_{i,x}^{10} & \psi_{i,x}^{01} \end{bmatrix} \tag{50}$$

such that

$$\epsilon(x) = Bu$$

and strain gradient-displacement matrix $(\mathbf{B_{SG}})_\mathbf{i}$ is

$$\mathbf{B_{SGi}} = \begin{bmatrix} \psi^{00}_{i,xx} & \psi^{10}_{i,xx} & \psi^{01}_{i,xx} & 0 & 0 & 0 \\ \psi^{00}_{i,xy} & \psi^{10}_{i,xy} & \psi^{01}_{i,xy} & 0 & 0 & 0 \\ \psi^{00}_{i,yy} & \psi^{10}_{i,yy} & \psi^{01}_{i,yy} & 0 & 0 & 0 \\ 0 & 0 & 0 & \psi^{00}_{i,xx} & \psi^{10}_{i,xx} & \psi^{01}_{i,xx} \\ 0 & 0 & 0 & \psi^{00}_{i,xy} & \psi^{10}_{i,xy} & \psi^{01}_{i,xy} \\ 0 & 0 & 0 & \psi^{00}_{i,yy} & \psi^{10}_{i,yy} & \psi^{01}_{i,yy} \end{bmatrix} \tag{51}$$

so that $\eta(x) = B_{SG}u$

where ψ^{00}, ψ^{10} and ψ^{01} are the three RKEM shape functions for node i.

Stress and conjugate stress can be written in vector form as

$$\sigma = \begin{bmatrix} \sigma_{xx} \\ \sigma_{yy} \\ \sigma_{xy} \end{bmatrix} \tag{52}$$

$$\tau = \begin{bmatrix} \tau_{xxx} \\ \tau_{xyx} \\ \tau_{yyx} \\ \tau_{xxy} \\ \tau_{xyy} \end{bmatrix} \tag{53}$$

For plane stress, the elastic modulus matrix ($\mathbf{D}$) that relates stress (σ) with strain(ϵ) is

$$\mathbf{D} = \frac{\mathbf{E}}{\mathbf{1} - \nu^\mathbf{2}} \begin{bmatrix} 1 & \nu & 0 \\ \nu & 1 & 0 \\ 0 & 0 & \frac{1-\nu}{2} \end{bmatrix} \tag{54}$$

where E and ν are Young's Modulus and Poisson's ratio, respectively

For 2D problem the matrix($\mathbf{D_{SG}}$ that relate τ with η) is given as

$$\mathbf{D_{SG}} = \begin{bmatrix} 2(a_1+a_2+ & 0 & (a_2+2a_3) & 0 & (a_2+2a_3) & 0 \\ a_3+a_4+a_5) & & & & & \\ 0 & (a_1+a_5 & 0 & (a_5+0.5a_2) & 0 & (a_1+0.5a_2) \\ & +2a_4) & & & & \\ 2(a_2+2a_3) & 0 & 2(a_3+a_4) & 0 & (a_2+2a_5) & 0 \\ 0 & (a_2+2a_5) & 0 & 2(a_3+a_4) & 0 & (a_2+2a_3) \\ (a_1+0.5a_2) & 0 & (a_5+0.5a_2) & 0 & (a_1+2a_4+ & 0 \\ & & & & a_5) & \\ 0 & (2a_1+2a_2) & 0 & (a_2+2a_3) & 0 & 2(a_1+a_2+ \\ & & & & & a_3+a_4+a_5) \end{bmatrix} \tag{55}$$

The matrix equivalent of the weakform is given as follows

$$\mathbf{Ku} = \mathbf{P} \tag{56}$$

Where $\mathbf{u}$ is a vector of nodal unknowns, $\mathbf{P}$ represents a set of loads applied at the nodes, and $\mathbf{K}$ is the stiffness matrix. Both $\mathbf{K}$ and $\mathbf{P}$ involve integrals over the problem domain. The integrands involve the basis functions or various of their derivatives and products of such functions.The stiffness matrix $\mathbf{K}$ can be written as sum of two stiffness matrix terms $\mathbf{K1}$ and $\mathbf{K2}$, $\mathbf{K1}$ corresponds to the first term on the left hand side of Eq. (46) while $\mathbf{K2}$ correspond to the second term on the left hand side of the same equation. The stiffness matrix term $\mathbf{K1}$ can be written as

$$\mathbf{K1} = \int_{\mathcal{B}} \mathbf{B^T}(\mathbf{x},\mathbf{y}) \cdot \mathbf{D} \cdot \mathbf{B}(\mathbf{x},\mathbf{y})\, \mathbf{dxdy}. \tag{57}$$

The stiffness matrix term $\mathbf{K2}$ can be written in this form

$$\mathbf{K2} = \int_{\mathcal{B}} \mathbf{B_{SG}}^{\mathbf{T}}(\mathbf{x},\mathbf{y}) \cdot \mathbf{D_{SG}} \cdot \mathbf{B_{SG}}(\mathbf{x},\mathbf{y})\, \mathbf{dxdy}. \tag{58}$$

The load vector P_i for node i because of traction load is given as

$$\mathbf{P} = \int_{\mathbf{\Omega}} \mathbf{N} \cdot \mathbf{t} \, \mathbf{d\Omega}. \tag{59}$$

where N is 6X2 matrix given as

$$N = \begin{bmatrix} \psi^{00} & 0 \\ \psi^{10} & 0 \\ \psi^{01} & 0 \\ 0 & \psi^{00} \\ 0 & \psi^{10} \\ 0 & \psi^{01} \end{bmatrix} \tag{60}$$

and

$$t = \begin{bmatrix} t_x \\ t_y \end{bmatrix} \tag{61}$$

where t_x and t_y traction in x and y direction.Point load can be added directly into Load Vector as in FEM.

Chapter 5

1D Examples

5.1 One-dimensional Toupin-Mindlin Strain Gradient Theory

Toupin and Mindlin included higher-order stresses and strains in their theory of linear elasticity, which serves today as the foundation of more advanced strain gradient plasticity formulations [29] [22] [8].Let us introduce a one-dimensional problem following their concepts. The solution for problem choosen in this section has been solved by C/DG method [21]

Let Ω be an open, bounded domain and Γ its boundary. Let Γ_g, Γ_q, Γ_t and Γ_r denote the displacement, displacement gradient, couple stress and traction boundaries, respectively.

The strong form of the problem can be written as

$$\sigma_{,x} - \bar{\sigma}_{,xx} + f = 0 \qquad in\ \Omega, \tag{62}$$

$$\phi = g \qquad on\ \Gamma_g \tag{63}$$

$$\phi_{,x}\dot{n} = q \qquad on\ \Gamma_q \tag{64}$$

$$\bar{\sigma} = r \qquad on\ \Gamma_r \tag{65}$$

$$(\sigma - \bar{\sigma}_{,x}\dot{n} = t \qquad on\ \Gamma_t \tag{66}$$

We have $\overline{\Gamma_g \bigcup \Gamma_t} = \Gamma$, $\Gamma_g \bigcap \Gamma_t = \emptyset$, $\overline{\Gamma_q \bigcup \Gamma_r} = \Gamma$, $\Gamma_q \bigcap \Gamma_r = \emptyset$, and f,g,q,r and t are given data. The constitutive equations for the stress σ and higher order stress $\bar{\sigma}$ can be expressed as

$$\sigma = \mu\psi_{,x}, \tag{67}$$

$$\bar{\sigma} = \mu l^2 \psi_{,xx}, \tag{68}$$

where μ is a material parameter and l is a length scale. We can write eq(62) to eq(66) with eq(67) and eq(68) as

$$(\mu\psi_{,x})_{,x} - (\mu l^2\psi_{,xx})_{,xx} + f = 0 \qquad in\ \Omega, \tag{69}$$

$$\phi = g \qquad on\ \Gamma_g \tag{70}$$

$$\phi_{,x}\dot{n} = q \qquad on\ \Gamma_q \tag{71}$$

$$\mu l^2\psi_{,xx} = r \qquad on\ \Gamma_r \tag{72}$$

$$\mu\psi_{,x} - (\mu l^2\psi_{,xx})_{,x}\dot{n} = t \qquad on\ \Gamma_t \tag{73}$$

From a mathematical point of view, the one-dimensional Toupin-Mindlin strain gradient theory is a generalization of the Bernoulli-Euler beam theory, involving in addition to the fourth-order derivative also a second order derivative.

5.2 Shear Layer Problem with the Toupin-Mindlin Theory

Toupin-Mindlin shear layer problem is considered as a model problem to validate our method(RKEM) for a strain gradient theory.Model problem its exact solution and convergence study is presented in this section. We want to simulate a shear-deformable body which is fixed on its left and upon which a traction acts on its right as shown in fig(4), in this problem the length from the attachment to where the traction acts is assumed to be L. The problem can be formulated as

$$(\mu\psi_{,x})_{,x} - (\mu l^2\psi_{,xx})_{,xx} + f = 0 \qquad in]0; L[, \tag{74}$$

$$\phi(0) = 0 \tag{75}$$

$$\phi_{,x}(0) = 0 \tag{76}$$

$$\phi_{,x}(L) = 0 \tag{77}$$

$$\mu\psi_{,x}(L) - \mu l^2\psi_{,xx}(L) = t \tag{78}$$

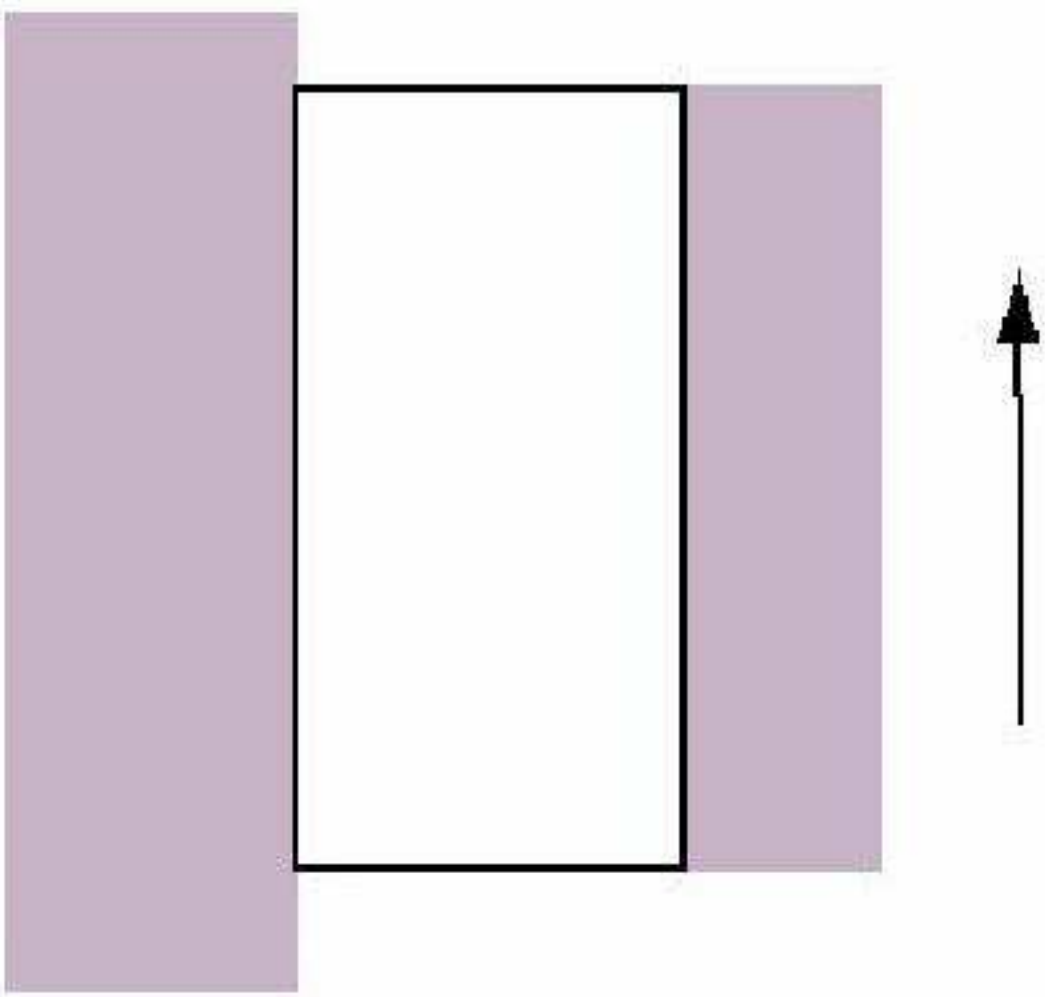

Figure 4. Shear layer attached on the left side (x =0) with traction acting on the right side (x=L)

5.2.1 Model Problem

The exact solution to this problem can be expressed as

$$\psi(x) = \frac{tl}{\mu(e^{\frac{L}{l}} + l)} \left(1 - e^{\frac{L}{l}} + e^{\frac{L-x}{l}} - e^{\frac{x}{l}}\right) + \frac{t}{\mu}x \tag{79}$$

The comparison of exact solution with RKEM solution is shown in Fig. (5) and plot of error(Exact solution - RKEM solution) is shown in Fig.(6)

5.2.2 Convergence Study

The convergence rates for interpolation can be seen in Fig.(7), where we have $N_{el} = \frac{1}{h}$. Rate of convergence in L_2 Norm is 3.5. Our numerical observations confirm our analytical results and order of interpolation considered lead to good rate of convergence in the L_2 Norm.

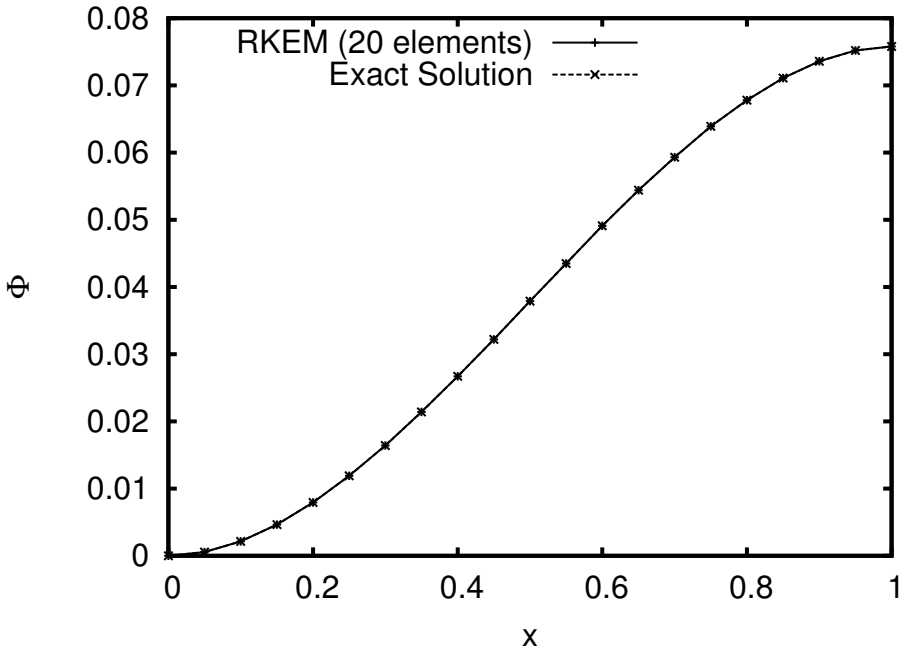

Figure 5. Exact solution vs RKEM solution for Toupin-Mindlin shear layer model problem

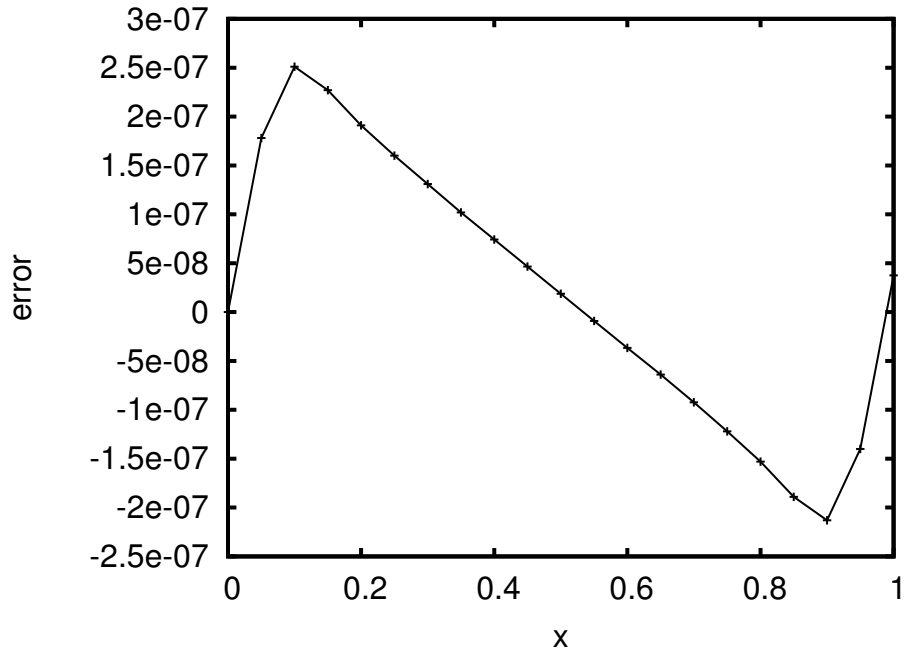

Figure 6. Error plot for Toupin-Mindlin shear layer model problem

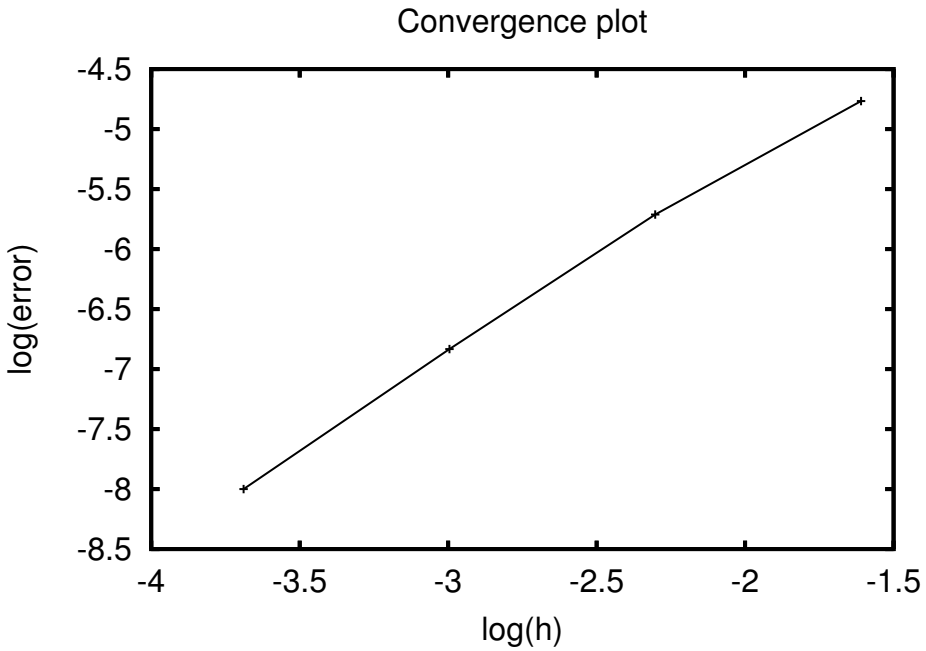

Figure 7. Convergence rate for RKEM L2P3I2 element

Chapter 6

2D Examples

6.1 Numerical Examples in Two Dimension

Due to the complexity and difficulity of a gradient theory, the obtainable analytical solutions are restricted to some simple problems.In this section we will focus on two problems :

1. Boundary layer analysis; and
2. The stress field analysis in an infinite plate, with a hole, subject to a bi-axial tension p at infinity, under a plane stress assumption.

6.1.1 Boundary Layer Analysis

Higher-order gradient theories predict the existence of a boundary layers adjacent to inhomogeneties such as interfaces. Consider, for example, a bimaterial composed of two perfectly bonded half planes of elastic strain gradient solids, subjected to remote shear stress σ_{12}^{∞} as shown in Fig(8).

6.1.2 Analytical Solution

An analytical solution is presented for a bimaterial, consisting of two perfectly bonded half planes of dissimilar linear elastic strain gradient solids. The bimaterial is subjected to a remote uniform shear stress σ_{12}^{∞} as shown in Fig(8). Here, we assume that material 1 lying below interface has a shear modulus μ_1, and an internal length scale l_1. while Material 2, lying above interface has a shear modulus μ_2, and an internal length scale l_2.

For this bimaterial system, conventional elasticity theory dictates that the shear stress is uniform and the shear strain jumps in magnitude at the interface from $\epsilon_{12} = \frac{\sigma_{12}^{\infty}}{2\mu_1}$ in material 1 to $\epsilon_{12} = \frac{\sigma_{12}^{\infty}}{2\mu_2}$ to material 2.

By including strain gradient effects, a continuously distributed shaer strain can be obtained. In this problem, the only non-zero displacement, strain, stress and higher order stress are $\mathbf{u}_1$,$\epsilon_1 2$,σ_{12} and τ_{221}, respectively, and they are functions of the co-ordinate x_2 only. From constitutive equation[6] and [7], it follows

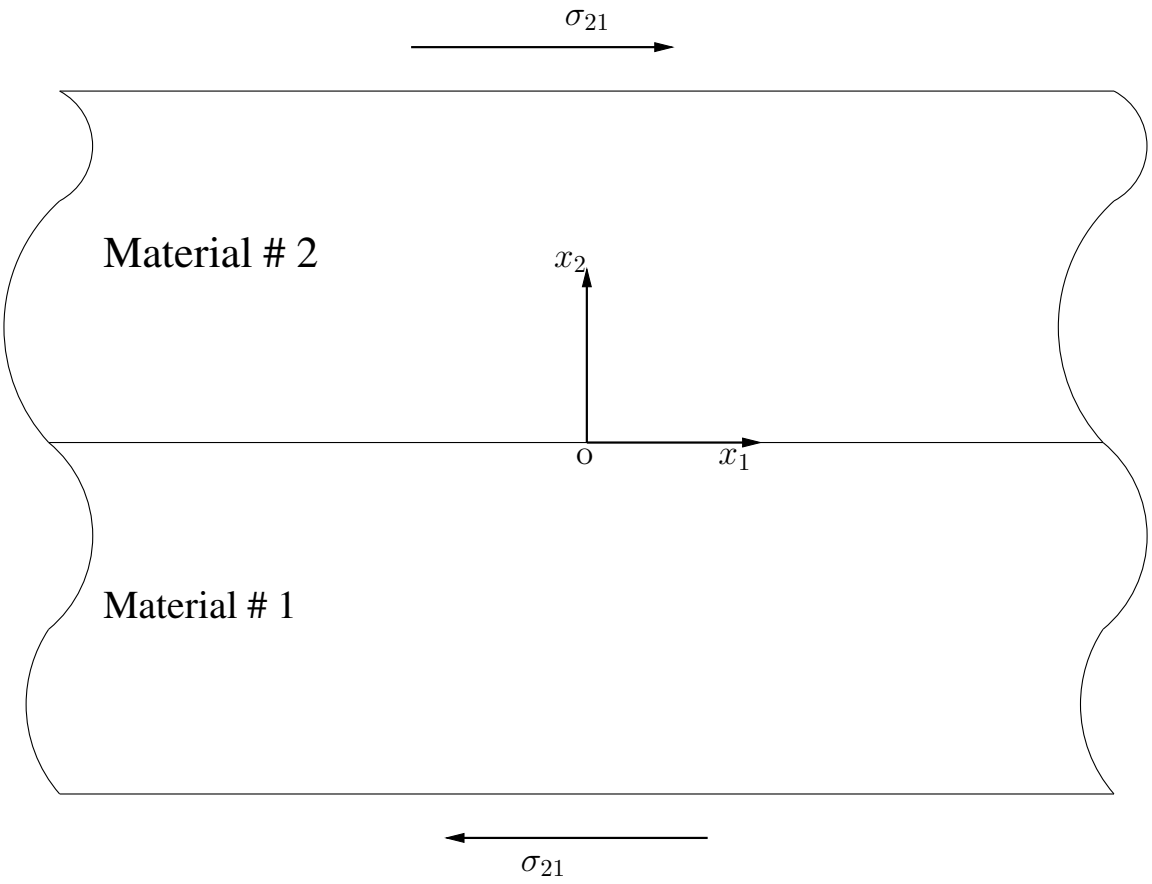

Figure 8. Geometry of a bimaterial under uniform shear

that

$$\sigma_{12} = 2\mu\epsilon_{12} \quad and \tau_{221} = 2\mu l_i^2 \eta_{221} = 4\mu l_i^2 \frac{\partial \epsilon_{12}}{\partial x_2} \tag{80}$$

in material i. Substitution of the above relation into the equilibrium equation[7] leads to

$$\frac{\partial \epsilon_{12}}{\partial x_2} - \hat{l_i}^2 \frac{\partial^3 \epsilon_{12}}{\partial {x_2}^3} = 0 \tag{81}$$

where $\hat{l_i} = \sqrt{2} l_i$. The general solution to the above ordinary diffrential equation is

$$\epsilon_{12} = d_1 + d_2 e^{\frac{x_2}{\hat{l_1}}} + d_3 e^{\frac{-x_2}{\hat{l_1}}} \qquad for x_2 < 0 \tag{82}$$

and

$$\epsilon_{12} = d_4 + d_5 e^{\frac{x_2}{\hat{l_2}}} + d_6 e^{\frac{-x_2}{\hat{l_2}}} \qquad for x_2 > 0 \tag{83}$$

Here d_1 to d_6 are 6 constants yet to be determined. The general solution is subjected to the following boundary condtions

1. $\epsilon_{12} \rightarrow \frac{\sigma_{12}^{\infty}}{2\mu_1}$ and $x_2 \rightarrow -\infty$ and $\epsilon_{12} \rightarrow \frac{\sigma_{12}^{\infty}}{2\mu_2}$ as $x_2 \rightarrow \infty$

   and at the interface

2. continuity of traction: $(\sigma_{21} - \tau_{221,2})|_{x_2 \rightarrow 0^-} = (\sigma_{21} - \tau_{221,2})|_{x_2 \rightarrow 0^+}$;

3. continuity of double stress traction $\tau_{221,2}|_{x_2 \rightarrow 0^-} = \tau_{221,2}|_{x_2 \rightarrow 0^+}$;

4. continuity of strain $\epsilon_{12}|_{x_2 \rightarrow 0^-} = \epsilon_{12}|_{x_2 \rightarrow 0^+}$

   The particular solution satisfying all these conditions is

$$\epsilon_{12} = \frac{\sigma_{12}^{\infty}}{2\mu_1} \left\{ 1 + \frac{\mu_1 - \mu_2}{\mu_2} \frac{\mu_2 \hat{l_2}}{\mu_1 \hat{l_1} + \mu_2 \hat{l_2}} e^{\frac{x_2}{\hat{l_1}}} \right\} \quad for\ x2 < 0 \tag{84}$$

$$\epsilon_{12} = \frac{\sigma_{12}^{\infty}}{2\mu_2} \left\{ 1 + \frac{\mu_2 - \mu_1}{\mu_1} \frac{\mu_1 \hat{l_1}}{\mu_1 \hat{l_1} + \mu_2 \hat{l_2} e^{\frac{-x_2}{\hat{l_2}}}} \right\} \quad for\ x2 > 0 \tag{85}$$

In a specific quantative example, we shall make the following arbitrary choice of constitutive parameters. The shear modulus μ of material 1 is taken as to be twice that of material 2. For each material, the constants a_3 and a_4 as defined in eq(5) are equal to $\frac{1}{2}\mu l^2$, while a_1,a_2 and a_5 vanish. Here l is usually called the internal length scale of materials with strain gradient effects.

Mesh for a typical problem is shown in Figure(9),size of domain is(1 X 1) or ($50lX50l$), where l is length scale boundary condition is of pure shear,beside this force boundary condition we set u=v=0 at left-bottom corner and v=0 at right-bottom corner to avoid the rigid movement.

Plot of shear strain ϵ_{12} for whole domain is given in Fig(10),Fig(11) is shear strain plot by conventional theory. A clear continious band along the interface is clear from comparison of these two plots.To make point more clear we have shown plot of shear strain along x=0.5 by both strain gradient and conventional theory in Fig(12) Fig(13) is comparison of analytical result and result obtained by RKEM, from this plot it is quite evident that solution by RKEM matches closely with analytical solutionThe L2 error for this problem were computed and plotted in Fig(14).The slope of line as determined by regression is 0.857

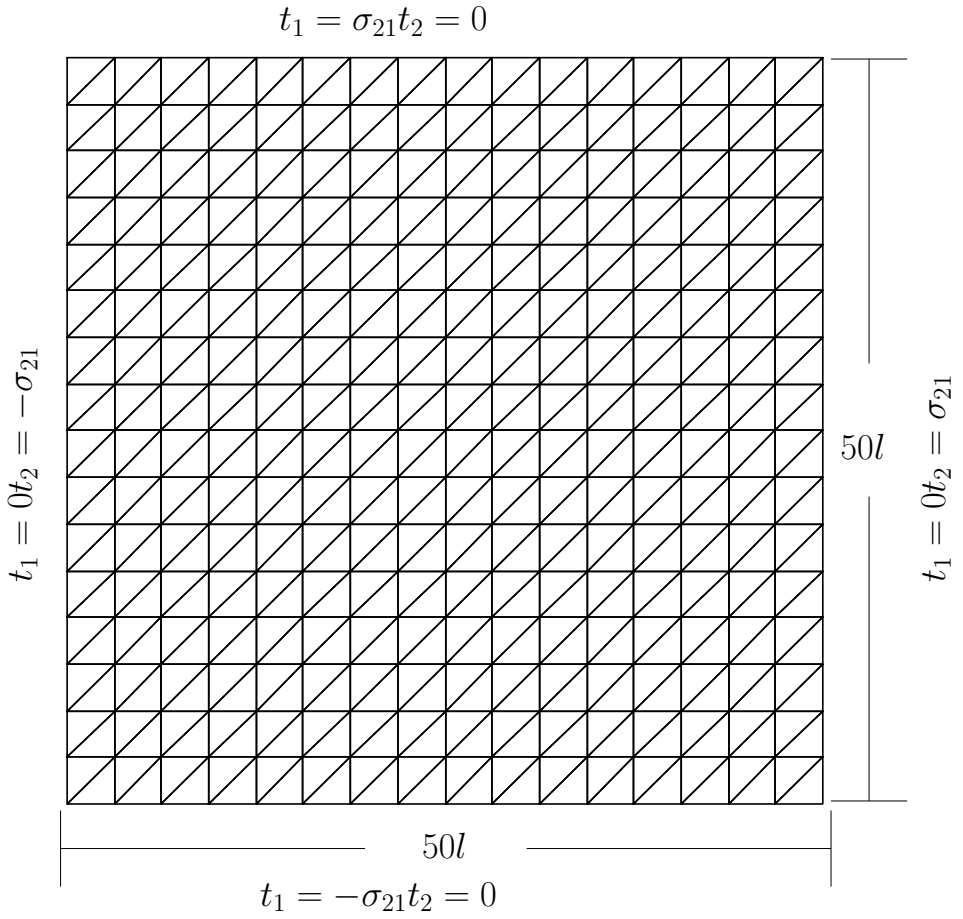

Figure 9. Mesh for bundary layer analysis

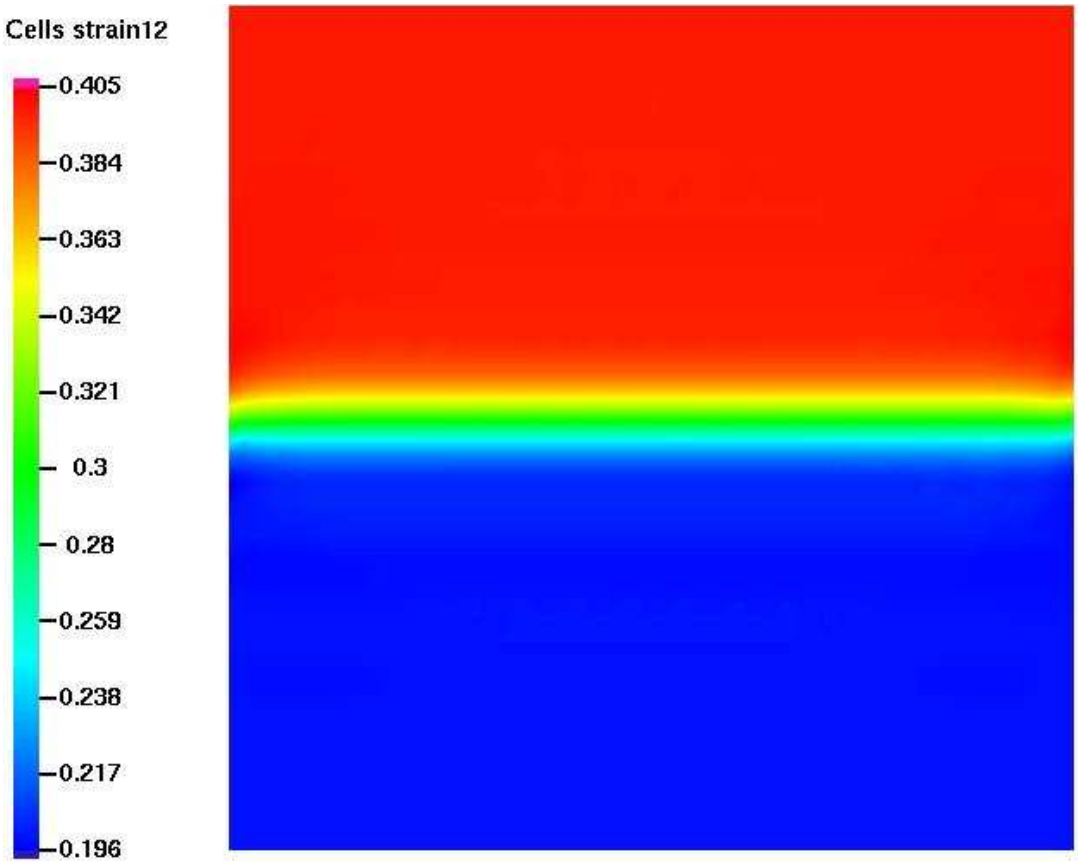

Figure 10. Shear strain plot by strain gradient theory

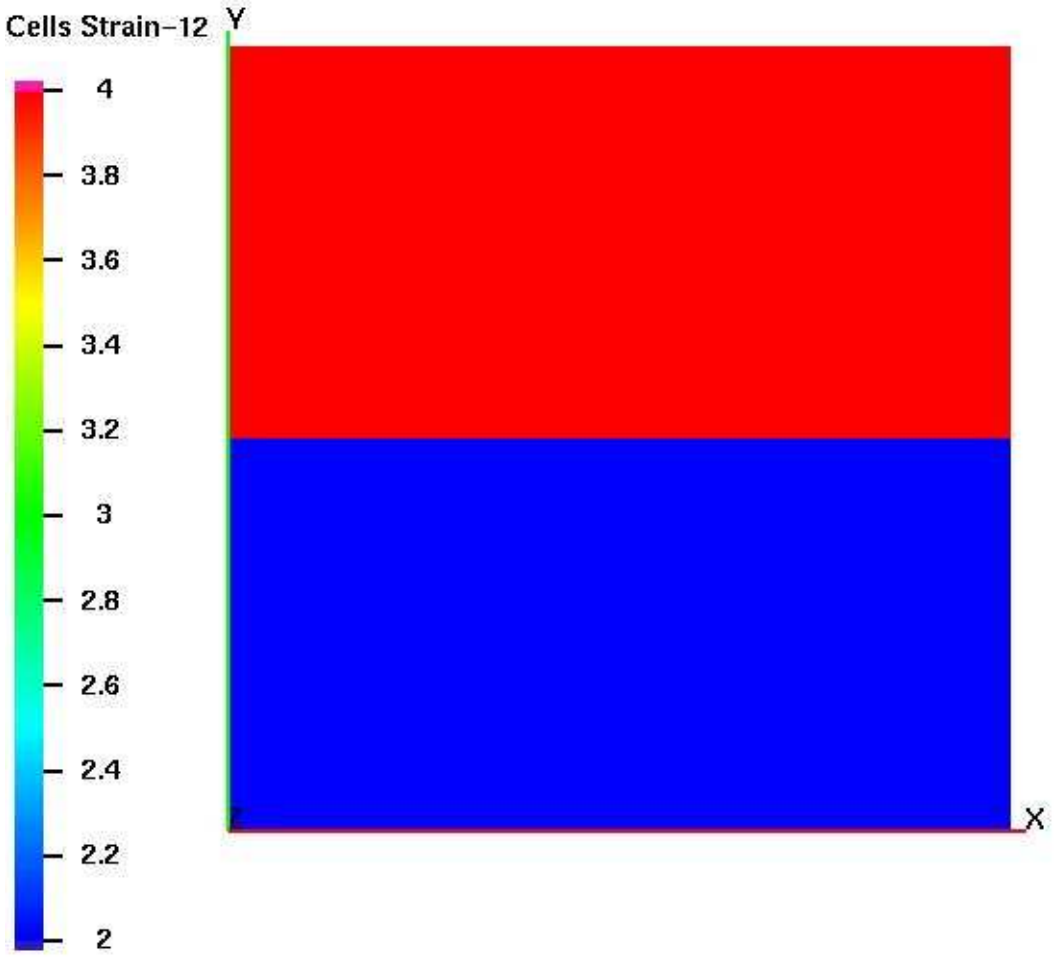

Figure 11. Shear strain plot by conventional theory

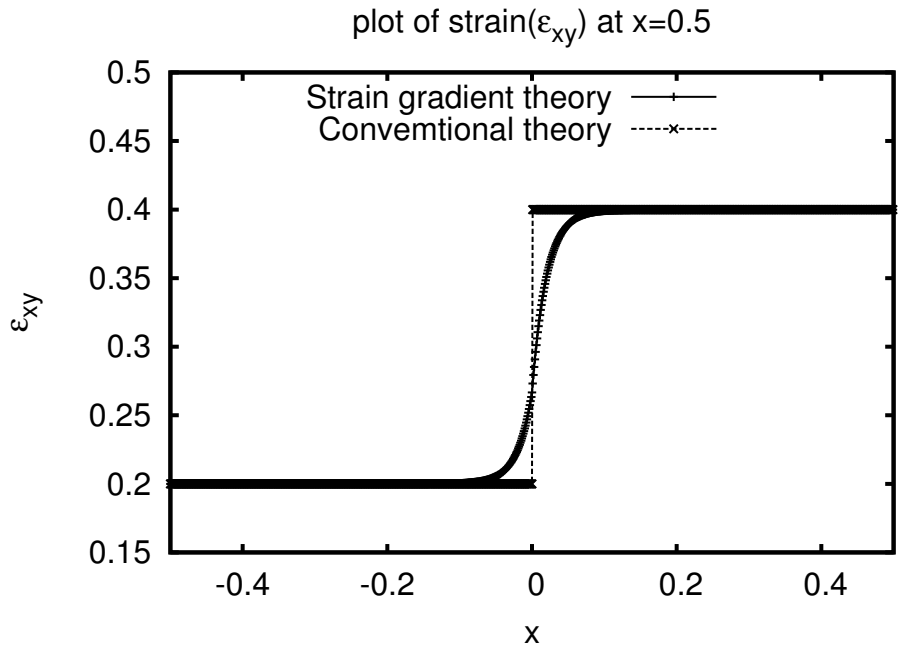

Figure 12. Comparison of strain gradient vs conventional theory

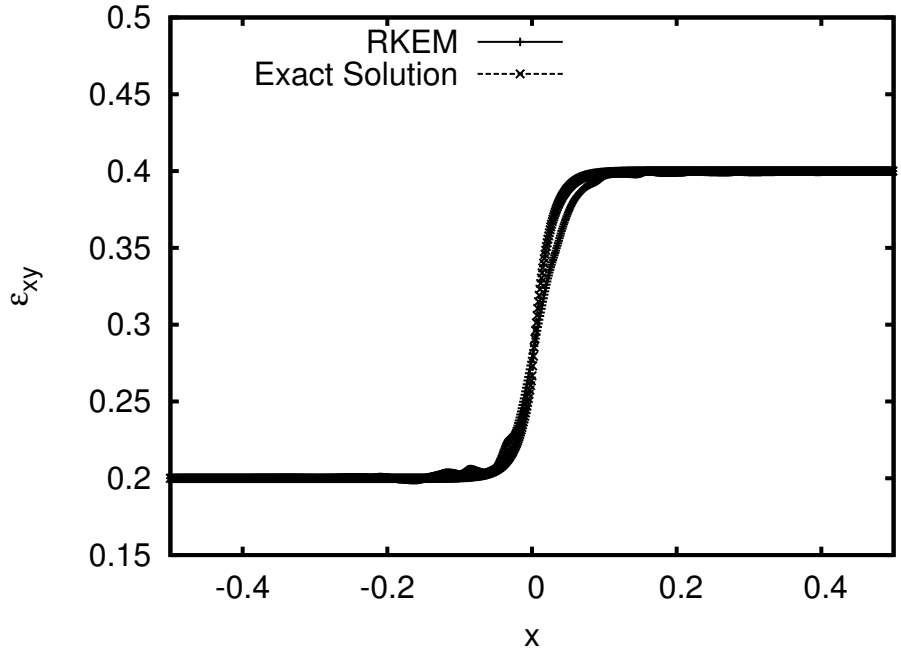

Figure 13. Comparison of exact solution vs RKEM solution

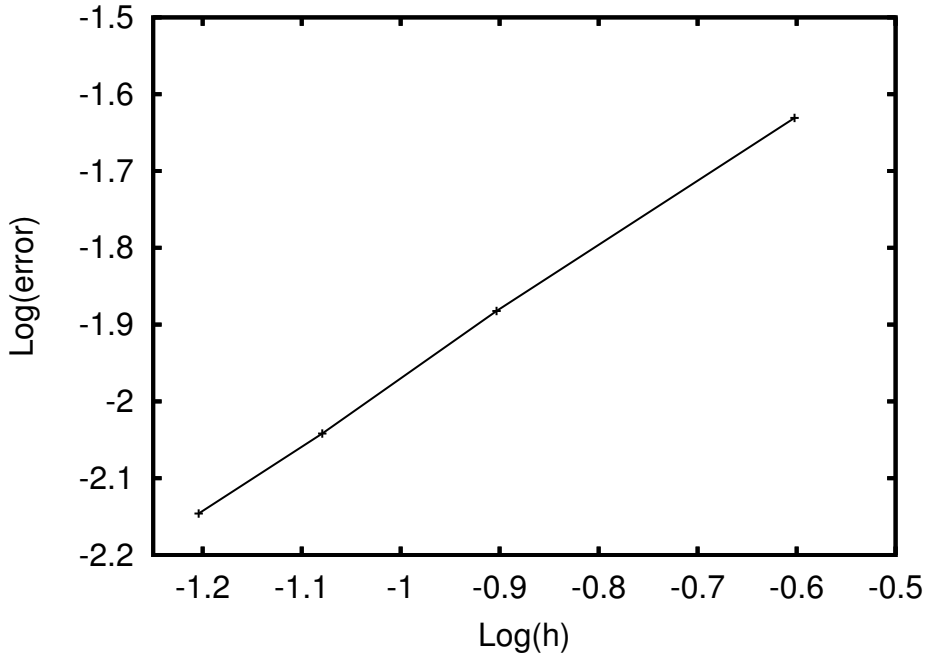

Figure 14. Convergence plot for RKEM solution)

6.2 An Infinite Plate With a Hole

In this section we consider the problem of an infinite plate with a hole of radius a subjected to a biaxial tension p at infinity under plane strain condition as shown in Fig(15). The constitutive model presented in chapter 2 is used to describe the mechancical response of the elastic material.

The problem is axially symmetric and the displacement field is of the form

u_r = u(r), $u_\theta = u_z = 0$,

where(r,θ,z) are cylindrical coordinates centered at center of the hole.

The exact solution of this problem has been developed by Exadaktylos [10] and is of the form

$$u(r) = \frac{p}{2G}\left\{(1-2\nu)r + \frac{a^2}{r} + \frac{l}{c}\left[\frac{a}{r}K_1(\frac{a}{l}) - (1-2\nu)K_1(\frac{r}{l})\right]\right\} \tag{86}$$

where

$$c = \frac{1-2\nu}{2}K_0(\frac{a}{l}) + \frac{1-\nu}{2}\left(\frac{4l}{a} + \frac{a}{l}\right)K_1(\frac{a}{l}) \tag{87}$$

and $K_n(x)$ are the well known modified Bessel functions of the second kind. The problem is solved numerically using the RKEM with T9P2I1 element. One quarter of the plate is analyzed because of symmetry; the

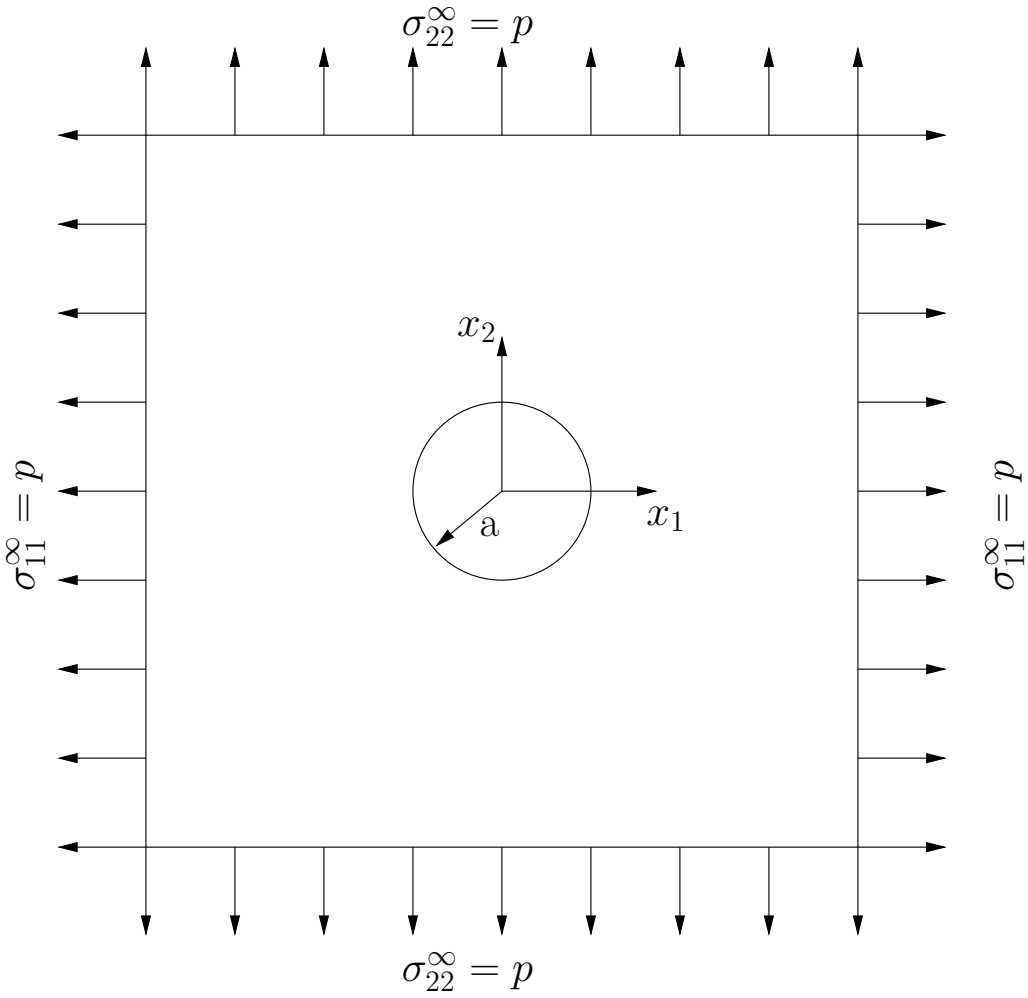

Figure 15. Notation and geometry of an infinite plate subjected to bi-axial remote tension

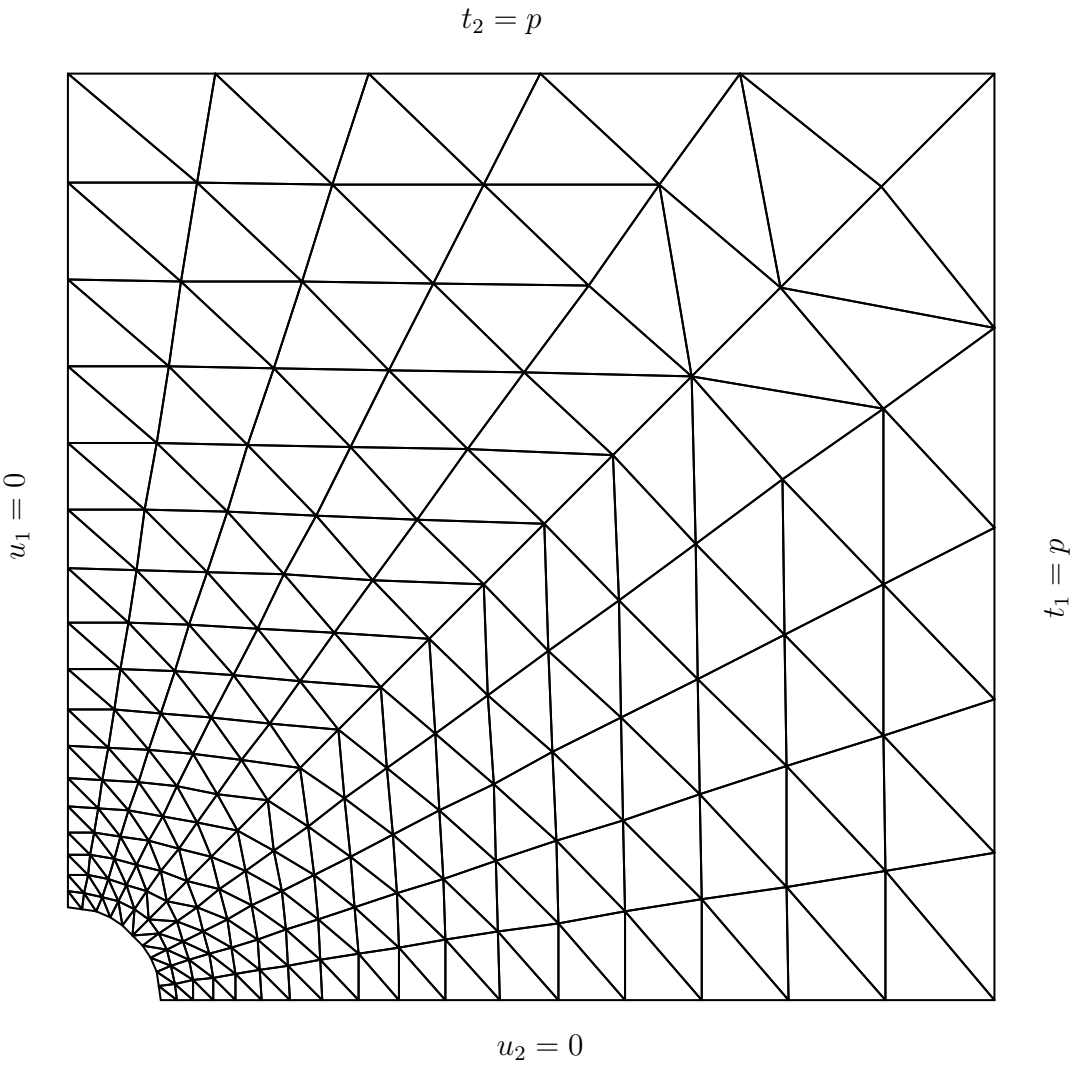

Figure 16. mesh for plate problem

mesh used for solving the problem is shown in Fig(16). The numerical calculations are carried out for ν = 0.3 and radius of hole(a) =3l, l is internal length scale of material. The size L of the domain analyzed is taken to be L = 10a. Since L is large compared to both a and l, the solution of this problem is expected to be close to that of an infinite plate.

Fig(17) is comparison of analytical result and result obtained by RKEM for plate problem, from this plot it is quite evident that solution by RKEM matches closely with analytical solution given in [**?**].

In Fig(18) and Fig(19) variation of σ_{rr} and $\sigma_{\theta\theta}$ has been shown respectively, these stress values are calculated along a radial line $\theta = 5^0$. From these result we can make conclusion for stress concentration

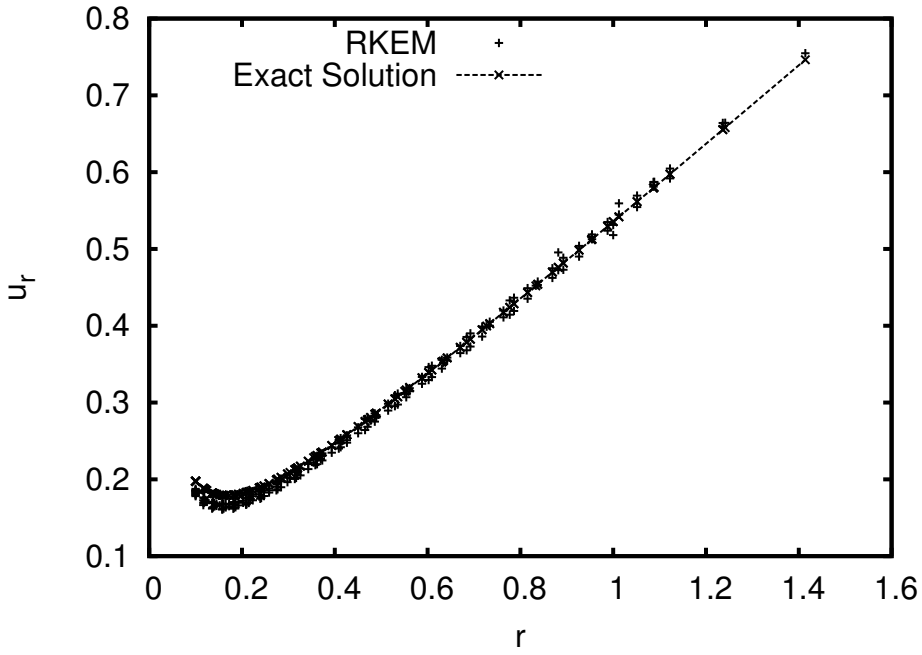

Figure 17. Variation of u_r for the plate with a hole

values, classical elasticity solution with l=0 predicts a stress concentration $\sigma_{\theta\theta}|_{r=a}$ = 2p and a value of $\sigma_{rr}|_{r=a}$ = 0, whereas the present elasticity solution with a =3l predicts $\sigma_{\theta\theta}|_{r=a}$ = 1.94p and $\sigma_{rr}|_{r=a}$ = 0.16p

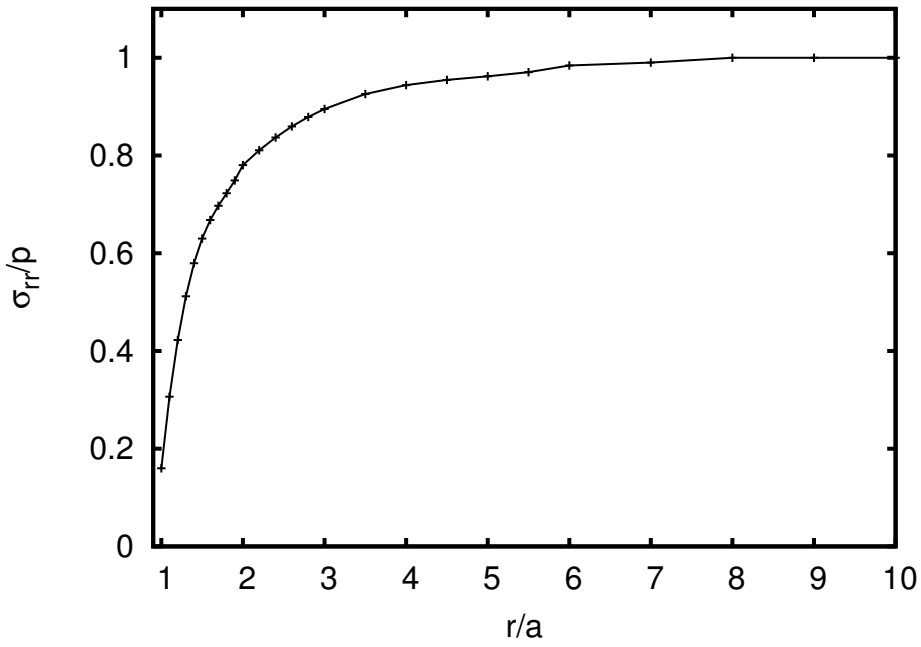

Figure 18. Variation of σ_{rr} for the plate with a hole

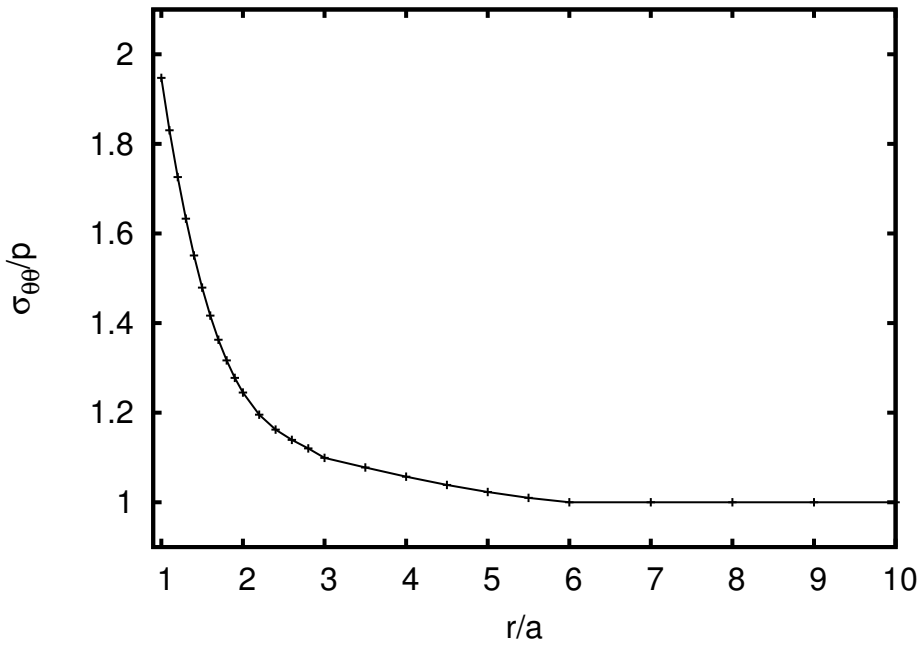

Figure 19. Variation of $\sigma_{\theta\theta}$ for the plate with a hole

Chapter 7

Conclusions

The Reproducing kernel Element Method(RKEM) has been developed for materials with the Toupin-Mindlin framework of strain gradient type constitutive theory. The good accuracy in these numerical simulations shows promising characteristics of RKEM for general problems of material in elasticity, where strain gradient effect may be important. The concepts and methods developed in this thesis are easily generalizable to other situations and offer the opportunity to derive new formulations for the new classes of problems and for problems abandoned in the past due to their complexity.

References

[1] G. Touzot B. Nayroles and P. Villon. Generalizing the finite element method: Diffuse approximation and diffuse elements. *Computational Mechanics*, 10:307–318, 1992.

[2] JT Oden C.Duarte. Hp-cloud - a meshless method to solve boundary-value problems. *Computer Methods in Applied Mechanics and Engineering*, 139:237–262, 1996.

[3] E. Cosserat and F. Cosserat. Theorie des corps deformables. *Hermann et Fils, Paris*, 1909.

[4] K. J. De, S.; Bathe. The method of finite spheres. *Computational Mechanics*, 25:329–345, 2000.

[5] F. Perazzo1 E. Oate and J. Miquel. A finite point method for elasticity problems. *Computers and Structures*, 79:2151–2163, 2001.

[6] E.Amanatidou and N.Aravas. Mixed finite element formulation of strain gradient elasticity problems. *Comput. Methods Appl. Mech. Engrg.*, 191:1723–1751, 2002.

[7] E.C.Aifantis. On the microstructural origin of certain inelastic models. *Trans. ASME J. Engng. Mater. Tech.*, 106:326–330, 1984.

[8] N. A. Fleck and J. W. Hutchinson. A phenomenological theory for strain gradient effects in plasticity. *J. Mech. Phys.Solids*, 41:1825–1857, 1993.

[9] N. A. Fleck and J. W. Hutchinson. Strain gradient plasticity. *Adv. Appl. Mech.*, 33:295–361, 1997.

[10] G.E.Exadaktylos. On the problem of the circular hole in an elastic material with microstructure,private communication.

[11] Y.Huang H.Gao and W.D.Nix. Mechanism based strain gradient plasticity ii. theory. *Journal of Mechanics and Physics of Solids*, 47:1239–1263, 1999.

[12] T.J.R. Hughes. *The Finite Element Method*. Dover, Mineola, New York, 2000.

[13] JM Melenk I.Babuska. The partition of unity method. *International Journal for Numerical Methods in Engineering"*, 40:727–758, 1997.

[14] H.Yuan J.Chen and F.H.Wittmann. Computational simulations of micro-indention tests using gradient plasticity. *CMES: Computer Modeling in Engineering and Science*, 3(6):743–754, 2002.

[15] J.Y.Shu and N.A.Fleck. Prediction of a size effect in micro indention. *International Journal of Solids and Structures*, 35:1363–1383, 1998.

[16] S. Li, H. Lu, W. Han, W. K. Liu, and D. C. Simkins, Jr. Reproducing kernel element method, Part II. Global conforming I^m/C^n hierarchy. *Computer Methods in Applied Mechanics and Engineering*, 193:953–987, 2004.

[17] W. K. Liu, W. Han, H. Lu, S. Li, and J. Cao. Reproducing kernel element method: Part I. Theoretical formulation. *Computer Methods in Applied Mechanics and Engineering*, 193:933–951, 2004.

[18] L.T.Tenek and E.C.Aifantis. A two-dimensional finite element implementation of a special form of gradient elasticity. *Computer Modelling in Engineering Science.(CMES)*, 3(6):731–742, 2002.

[19] H. Lu, S. Li, D. C. Simkins, Jr., W. K. Liu, and J. Cao. Reproducing kernel element method Part III. Generalized enrichment and applications. *Computer Methods in Applied Mechanics and Engineering*, 193:989–1011, 2004.

[20] L.B. Lucy. A numerical approach to the testing of the fission hypothesis. *The Astronomical Journal*, 82:1013–1024, 1977.

[21] G.Engel K.Garikipati T.J.R. Hughes M.G. Larson L. Mazzei and R.L. Taylor. Continuous/discontinuous finite element approximations of fourth-order elliptic problems in structural and continuum mechanics with applications to thin beams and plates, and strain gradient elasticity. *Computer Method in Engineering Science.*, 191:3669–3750, 2002.

[22] R.D. Mindlin. Micro-structure in linear elasticity. *Arch. Rational Mech. Anal.*, 16:51–78, 1964.

[23] O.C.Zienkiewicz and R.L.Taylor. *The Finite Element, 4th Edition*. McGraw-Hill, New York, 1994.

[24] D. C. Simkins, Jr., S. Li, H. Lu, , and W. K. Liu. Reproducing kernel element method Part IV. Globally compatible $C^n(n \geq 1)$ triangular hierarchy. *Computer Methods in Applied Mechanics and Engineering*, 193:1013–1034, 2004.

[25] Daniel C. Simkins, Jr. *General Reproducing Kernel Element Hierarchies*. PhD thesis, University of California, Berkeley, CA, May 2004.

[26] T.Zhu S.N.Atluri. A new meshless local petrov-galerkin(mlpg) approach in computational mechanics. *Computational Mechanics*, 22:117–127, 1998b.

[27] B. Specht. Modified shape functions for the three node plate bendinf element passing the patch test. *International Journal of Numerical Methods and Engineering*, 26:705–715, 1988.

[28] L.Gu T.Belytschko, YY Lu. Element-free galerkien methods. *International Journal for Numerical Methods in Engineering"*, 37:229–256, 1994.

[29] R. A. Toupin. Elastic materials with couple stresses. *Arch. Rational Mech. Anal.*, 11:385–414, 1962.

[30] J.Y.Shu W.E.King and N.A.Fleck. Finite elements for material with strain gradient effects. *International Journal for Numerical Methods in Engineering*, 44:373–391, 1999.

[31] W.D.Nix Y.Huang, H.Gao and J.W.Hutchinson. Mechanism based strain gradient plasticity ii. analysis. *Journal of Mechanics and Physics of Solids*, 48:99–128, 2000.

[32] Z.C.Xia and J.W.Hutchinson. Crack tip field in strain gradient plasticity. *Journal of Mechanics and Physics of Solids*, 44:1621–1648, 1996.

[33] S.Chen Z.Tang and S.N.Atluri. Analysis of materials with strain-gradient effects:mlpg approach with nodal displacement only. *Computer Modelling in Engineering Science.(CMES)*, 4(1):177–196, 2003.